



Article

Experimental Validation of a Bidirectional Multilevel dc–dc Power Converter for Electric Vehicle Battery Charging Operating under Normal and Fault Conditions

Vitor Monteiro , Catia F. Oliveira and Joao L. Afonso 

ALGORITMI Research Centre/LASI, University of Minho, 4800-058 Guimarães, Portugal

* Correspondence: vmonteiro@dei.uminho.pt

Abstract: This paper presents a bidirectional multilevel dc–dc power converter for electric vehicle (EV) battery charging. The operating principle of the power converter was presented, analyzed, and experimentally validated under normal and fault conditions. The topology under study was integrated into a bipolar dc grid through the split dc-link of the bidirectional multilevel dc–dc power converter. Considering the failures that can occur in the bipolar dc grid, i.e., in each wire of the bipolar dc grid (positive, negative, and neutral), it was experimentally verified that the dc–dc power converter ensures that the EV battery-charging process continues, regardless of the occurrence or absence of open-circuit failures. In light of this fact, the proposed control algorithms and the presented topology were validated through a set of considerable simulation and experimental results, analyzing the distinct states of the power semiconductors, which compose the bidirectional multilevel dc–dc power converter, for distinct conditions of operation. The developed laboratory prototype of the bidirectional multilevel dc–dc power converter for EV battery charging, which was implemented to obtain the experimental results, is described in detail in this paper. The experimental validation was carried out for the main different fault conditions in the bipolar dc grid in terms of open-circuit failures and, moreover, considering the steady-state and transient-state operations of the dc–dc power converter. The experimental analysis demonstrated that even in the presence of failures in the positive, negative, or neutral wires of the bipolar dc grid, the bidirectional multilevel dc–dc power converter guarantees the correct EV battery-charging operation.

Keywords: fault tolerance analysis; open-circuit failures; multilevel dc–dc power converter; EV battery charging; bipolar dc grid



Citation: Monteiro, V.; Oliveira, C.F.; Afonso, J.L. Experimental Validation of a Bidirectional Multilevel dc–dc Power Converter for Electric Vehicle Battery Charging Operating under Normal and Fault Conditions. *Electronics* **2023**, *12*, 851. <https://doi.org/10.3390/electronics12040851>

Academic Editor: Carlos

Andrés García-Vázquez

Received: 23 December 2022

Revised: 16 January 2023

Accepted: 6 February 2023

Published: 8 February 2023



Copyright: © 2023 by the authors. Licensee MDPI, Basel, Switzerland. This article is an open access article distributed under the terms and conditions of the Creative Commons Attribution (CC BY) license (<https://creativecommons.org/licenses/by/4.0/>).

1. Introduction

Concerning the minimization of greenhouse gas emissions and with the increasing prices of fossil fuels, the adoption of new alternatives to vehicles with internal combustion engines is fundamental. In this context, with growing technological development, electric vehicles (EVs) represent a viable alternative within the transportation sector, where innovative charging stations are gaining preponderance without neglecting power quality [1,2]. Furthermore, dc grids have also contributed to a cleaner environment due to the fact that this type of grid, which has a reduced number of power converters, allows for not only EV interface, but also the integration of energy storage systems (ESS)—namely stationary batteries—and renewable energy sources (RES), such as photovoltaic panels and wind turbines [3,4]. More specifically, dc grids present two main configurations: unipolar and the bipolar dc grids [5]. Regarding unipolar dc grids, the necessary control is not complex compared with bipolar dc grids; however, unipolar grids consist of only two wires, carrying one dc voltage level. On the other hand, in the case of bipolar dc grids, they are composed of three different dc voltage levels, $+v_{dc}$, 0, and $-v_{dc}$, allowing the integration of power converters of different voltage levels [6,7]. Despite that, the connection of different loads

can lead to an unbalanced system, and the control necessary for this type of dc grid is complex [8]. However, in the occurrence of failures in one wire of the dc grid, the system can continue operating through the power supplied by the two wires, representing an attractive advantage when compared with unipolar dc grids. Regarding the integration of EVs for performing battery charging, many topologies have been implemented, as described in the review of on-board EV chargers presented in [9], in the multifunction off-board EV charger in smart homes presented in [10], in a Vienna rectifier for EV battery chargers presented in [11], in a converter with multiple operation modes for EV chargers presented in [12], in the multiport series-resonant dc–dc converters presented in [13], and in the complete review of EV technologies, battery-charging strategies, standards, and optimization techniques presented in [14]. However, the occurrence of failures in power converters can damage the equipment connected to the dc grid or other electrical components. Specifically, an overview concerning fault management for EV on-board chargers was presented in [15], and the influence of fault ride-through ability on EV charging stations in critical voltage conditions was presented in [16]. Regarding the failures that can occur in power electronics converters, most failures originate in the capacitors, the circuit drivers, and the power semiconductors that compose the power converters, as demonstrated in [17] for dc–dc converters in dc microgrids, and in [18] for a specific dual active bridge dc–dc converter. Regarding the failures that can occur in the power grid, the most critical failure is related to power outages. In case of bipolar dc grids, a failure can occur in any of the three wires (e.g., if a failure occurs in the negative wire, a system linked to the positive or neutral wire is not affected by such failure). For this reason, the development of fault tolerance power electronics converters aiming to minimize the impact of such failures originating in dc grids is extremely important [19,20]. In the case of EV battery chargers, the occurrence of failures can compromise EV battery charging, especially if the power converters are not fault tolerant; i.e., despite the presence of failures, the fault tolerance feature avoids interrupting system operation until the repair is carried out, as demonstrated in [21], and more fully explained in the review of fault diagnosis analysis for dc–dc converters presented in [22]. As mentioned, the occurrence of failures can be in the dc wires of dc grids, where the dc-link capacitors of the dc–dc power converter connected to the dc grid can be also damaged [23]. In a bipolar dc grid, whose constitution is based on three different wires (positive, negative, and neutral), a failure in one wire of the bipolar dc grid affects, for example, the dc-link voltage of the power converter it is connected to. In view of this fact, fast detection and actuation of the failure is crucial to not deteriorate the power converter or the entire system. In the literature, several fault detection algorithms for dc–dc power converters can be found; however, some algorithms require additional hardware, such as voltage or current sensors and power semiconductors, making this solution more expensive [24]. To reduce costs, fault detection algorithms that do not require extra sensors are being investigated. In light of this, these algorithms select diagnostic variables; namely, the inductor current [25], the diode voltage [26], or the input voltage [27]. However, the main disadvantages of some fault detection algorithms are their complexity and the fact that some algorithms are designed for a specific type of power converter [28].

In this paper, bidirectional multilevel dc–dc power converter is presented and used as EV battery charger operating under normal and fault conditions Figure 1. presents the conventional configuration of a bipolar dc grid, emphasizing the contextualization of such a power converter. Therefore, as our main contributions are as follows: (i) a fault analysis that considers the operation of the dc–dc power converter in the presence of failures in the positive, negative, or neutral wires of the bipolar dc grid (i.e., when the failures occurs in the dc bipolar grid); (ii) a fault analysis that maintains the operation of the power converter without using any additional hardware, such as sensors or power semiconductors; (iii) a dc–dc power converter that guarantees the EV battery-charging operation, despite the presence of failures on the bipolar dc grid; (iv) a detailed analysis of the bidirectional multilevel dc–dc converter, carried out under normal and fault conditions, and considering steady-state and transient-state operation in both normal and fault conditions; (v) a proposed control

strategy applied to the bidirectional multilevel dc–dc power converter in both normal and fault conditions; (vi) experimental validation considering all the main conditions of operation under normal and fault conditions with a developed laboratory prototype. The topology of the bidirectional multilevel dc–dc power converter for EV battery charging, integrated in a bipolar dc grid, is presented in Figure 2.

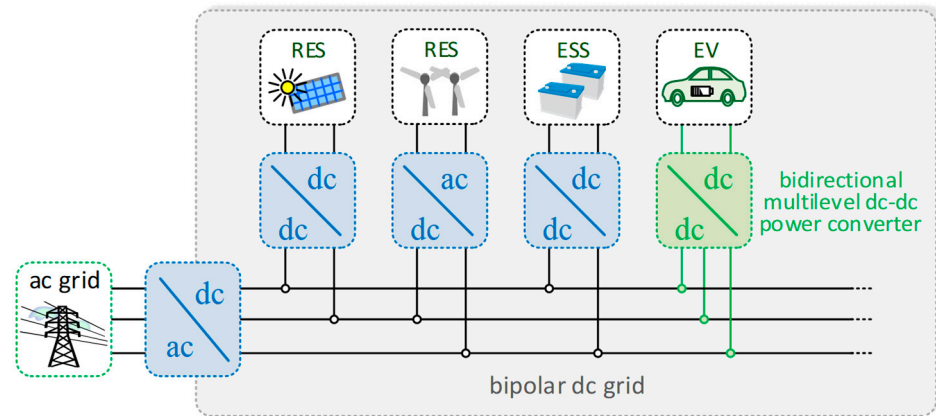


Figure 1. Conventional configuration of a bipolar dc grid, emphasizing the contextualization of the bidirectional multilevel dc–dc power converter for EV battery charging.

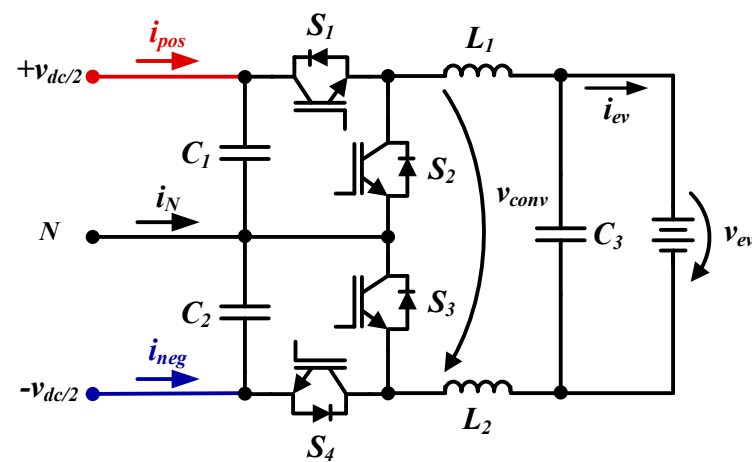


Figure 2. Bidirectional multilevel dc–dc power converter for EV battery charging integrated in a bipolar dc grid.

This paper is organized as follows: Section 2 describes the operating principle of the proposed bidirectional multilevel dc–dc power converter under normal and fault conditions. Section 3 presents the simulation results of the bidirectional multilevel dc–dc converter for EV battery charging under normal and fault conditions in a bipolar dc grid. Section 4 presents the developed laboratory prototype used to obtain the experimental results, corroborating the simulations results described in the previous section. Finally, in Section 5, the main conclusions are presented.

2. Description of the Multilevel dc–dc Power Converter

The proposed bidirectional multilevel dc–dc power converter aims to guarantee correct EV battery charging, allowing the battery-charging process to function based on dedicated digital control algorithms of constant current and constant voltage. However, failures can occur in the bipolar dc grid—namely, open-circuit faults where the EV charger is connected—which can compromise the EV battery-charging operation. Thus, this section describes the operating principle of the bidirectional multilevel dc–dc power converter under normal conditions and in the presence of faults, which can occur during the EV

battery charging. Regarding the occurrence of failures in the bipolar dc grid, in this section are presented three different failures: in the positive, neutral, and negative wires of the dc grid. Moreover, the proposed control strategy applied in normal and fault conditions for EV battery charging is described in detail. Figure 3 shows the block diagram of the control strategy applied to the bidirectional multilevel dc–dc power converter.

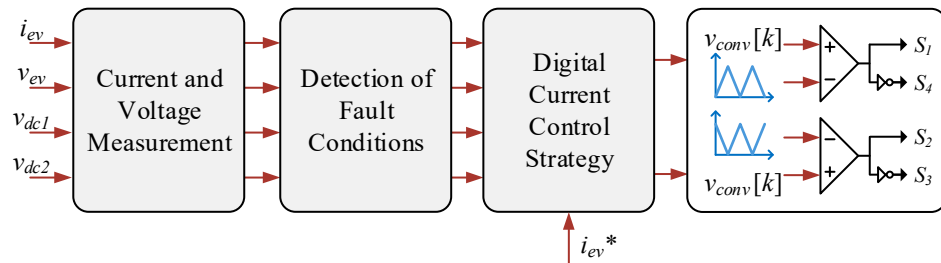


Figure 3. Block diagram of the control strategy applied to the bidirectional multilevel dc–dc power converter.

2.1. Multilevel dc–dc Power Converter Operation under Normal Conditions

In this paper, the proposed bidirectional multilevel dc–dc power converter was analyzed when operating as EV battery charger, which corresponds to the buck-mode operation. This topology consists of four IGBTs, a passive filter (LC), and a split dc-link. In the buck-mode operation, the multilevel dc–dc power converter can produce three voltage levels depending on the dc-link voltages and the battery voltage; namely the voltage levels 0, $+v_{dc}/2$, and $+v_{dc}$. In terms of operation principle, the dc–dc converter produces a voltage level of 0 when the power semiconductors S_1 and S_4 are disabled and the current flows through the antiparallel diodes of the semiconductors S_2 and S_3 . In this case, the energy of the inductors L_1 and L_2 was used for the EV battery charging. On the other hand, the output voltage is $+v_{dc}/2$ in two different conditions: (a) when only the semiconductor S_1 is enabled and the inductors L_1 and L_2 , as well as the EV battery, are charged through the capacitor C_1 ; or (b) when only the semiconductor S_4 is enabled and the inductors L_1 and L_2 and the EV battery are charged through the capacitor C_2 . The output voltage of the dc–dc power converter is $+v_{dc}$ when the power semiconductors S_1 and S_4 are enabled and the inductors L_1 and L_2 and the EV battery are charged through the capacitors C_1 and C_2 .

Figure 4 presents the correlation among the duty cycle and the normalized current ripple on the inductor of the bidirectional multilevel dc–dc power converter, both for the buck mode and boost mode. During the buck mode, as shown, the duty cycle ratio between 0 and 50% and between 50% and 100% is symmetrical. In this case, the current ripple presents higher duty cycle values at around 25% and 75%, and, on the other hand, lower duty cycle values at around 0%, 50%, and 100%. During the boost mode, as shown, the current ripple is almost constantly greater between 50% and 100% than between 0 and 50%. The current ripple has lower duty cycle values close to 0 and 50%, and higher duty cycle values close to 100%.

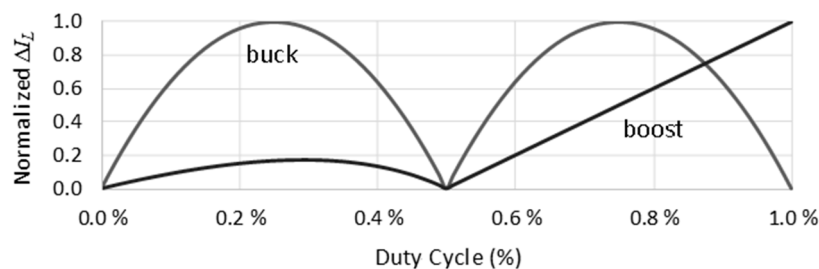


Figure 4. Correlation between the duty cycle and the normalized current ripple for the inductor of the bidirectional multilevel dc–dc power converter, considering the buck mode and boost mode.

2.2. Multilevel dc–dc Power Converter Operation under Fault Conditions

As previously mentioned, in this paper three types of failures that can occur in the bipolar dc grid were considered and analyzed; namely, failures in the positive, negative, and neutral dc wires. In this paper, the faults were identified by measuring the voltages on the bipolar dc grid side, i.e., the voltages across the capacitors C_1 and C_2 . Since such voltages are continuously measured by the digital control platform, it is easy to identify when a fault occurs. In such circumstances, the power converter is not responsible for taking any action to solve the faults, since the fault occurs from the point of view of the bipolar dc grid. Analysis concerning the probability of occurrence of such faults is outside the scope of this paper, since the main objective was to present an experimental validation of a bidirectional multilevel dc–dc power converter under fault conditions.

For each failure in the bipolar dc grid, there are two different operation modes. In case of a failure in the positive wire of the bipolar dc grid, the semiconductor S_1 ceases to operate, so the EV battery is charged through either the energy of capacitor C_2 or the energy stored by the inductors L_1 and L_2 . Figure 5 presents the operation principle of the multilevel dc–dc converter under fault conditions connected to a bipolar dc grid. In the first case, the current flows through the antiparallel diode of S_2 and the semiconductor S_4 , as illustrated in Figure 5a. The output voltage of the dc–dc converter is $+v_{dc}/2$. In the second case, the current flows through the antiparallel diodes of S_2 and S_3 , and the output voltage of the dc–dc converter is 0 V (Figure 5d). In the presence of a failure in the negative wire of the bipolar dc grid, there is no energy from the capacitor C_2 , and the semiconductor S_4 is not operational. However, the EV battery is charged through either the energy of the capacitor C_1 or the inductors L_1 and L_2 . In the first case, the current flows through the semiconductor S_1 and the antiparallel diode of S_3 , and the output voltage of the dc–dc converter is $+v_{dc}/2$ (Figure 5b). In the second case, the output voltage is 0 V and the current flows through the antiparallel diodes of S_2 and S_3 (Figure 5d). In the presence of a failure in the neutral wire of the bipolar dc grid, the EV battery is charged through either the energy of the capacitors C_1 and C_2 or the inductors L_1 and L_2 . Regarding the first case, the dc–dc converter produces a voltage value of $+v_{dc}$ since the semiconductors S_1 and S_4 are switching, and the energy comes from both capacitors of the dc-link, as represented in Figure 5c. In the second case, the semiconductors S_1 and S_4 are disabled, and the current flows through the antiparallel diodes of S_2 and S_3 (Figure 5d), whose output voltage, as produced by the dc–dc converter, is 0 V.

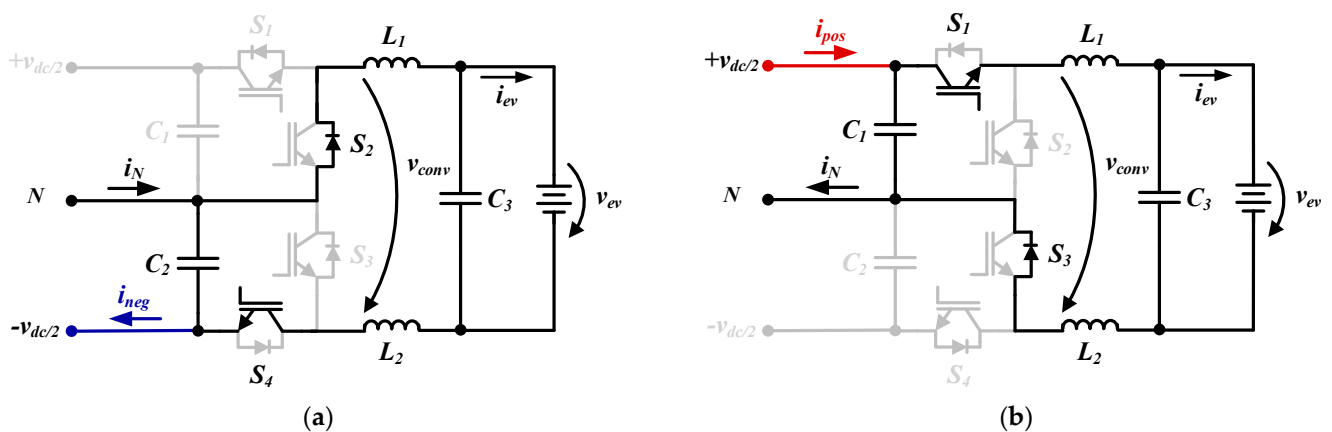


Figure 5. Cont.

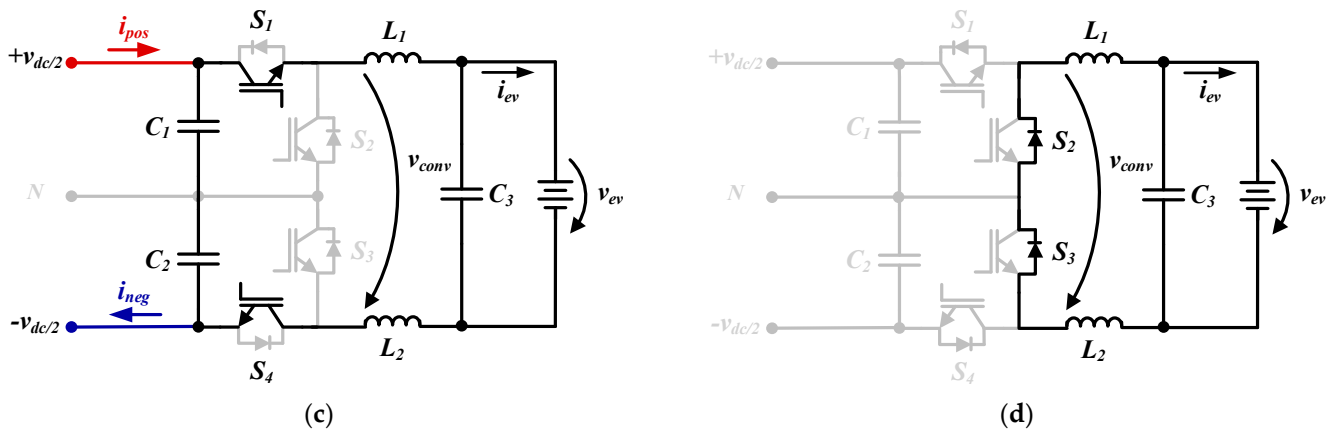


Figure 5. Operation principle of the multilevel dc–dc converter under fault conditions connected to a bipolar dc grid: (a) failure in the positive wire of the bipolar dc grid; (b) failure in the negative wire of the bipolar dc grid; (c) failure in the neutral wire of the bipolar dc grid; (d) common operation mode to the mentioned three failures.

2.3. Operation Principle of the Control Strategy Applied in Normal and Fault Conditions

This section presents the operation principle of the proposed control strategy used for EV battery charging, which was applied in two different situations: normal and fault conditions. Equation (1) is the equation that determines the output voltage of the dc–dc power converter, which corresponds to the voltage that the converter must produce in order to obtain the desired current for charging the EV battery:

$$v_{conv} = v_{L1} + v_{ev} + v_{L2}, \tag{1}$$

where v_{L1} and v_{L2} correspond to the voltages in inductors L_1 and L_2 , respectively. According to Figure 2, the voltage measured in the EV battery is represented by v_{ev} . Knowing that the current measured in the inductors L_1 and L_2 is the same, Equation (1) can be represented by the following equation:

$$v_{conv} = v_{ev} + (L_1 + L_2) \frac{di_{ev}}{dt}. \tag{2}$$

Equation (2) corresponds to the main control law of the multilevel dc–dc converter. Therefore, it must be digitally implemented. For this purpose, the forward Euler approximation was applied for the derivative, and the other variables were measured and acquired by the ADC at the beginning of each sampling period of the main control cycle. The value of the coupling filter is a digital value, defined according to the measured value from a digital multimeter. Therefore, Equation (3) shows the digital implementation of the output control variable of the control strategy (v_{conv}), where T_s corresponds to the sampling period (defined in the digital control by a timer interruption), the reference current is represented by $i_{ev}[k+1]$, and the EV battery current is represented by $i_{ev}[k]$:

$$v_{conv} [k] = v_{ev} [k] + \frac{L_1 + L_2}{T_s} (i_{ev}[k + 1] - i_{ev}[k]). \tag{3}$$

After the digital implementation of Equation (3), the variable v_{conv} was multiplied by the peak value of the triangular carrier and subsequently divided by the total value of the dc-link voltage (on the dc grid side). Then, the result was directly compared with two triangular, 180° phase-shifted carriers, whose comparison resulted in the control signals of the semiconductors S_1 and S_4 . The advantage of using two triangular, 180° phase-shifted carriers is the reduced ripple of i_{ev} , whose frequency is double of the established switching frequency [29]. This is a relevant fact, since it permits the design of coupling filters with reduced values, and consequently, smaller sizes, when compared with the traditional

dc–dc buck converters. As a result, the multilevel dc–dc converter operates with the same principle of operation as an interleaved converter, which presents an additional advantage. The current control scheme applied to the bidirectional multilevel dc–dc power converter is presented in Figure 6.

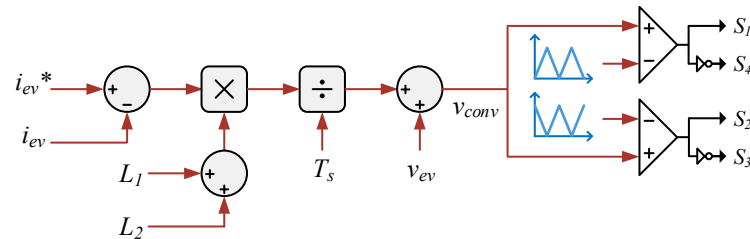


Figure 6. Current control scheme applied to the bidirectional multilevel dc–dc power converter.

3. Computational Validation

Following the detailed description of the operation principle of the multilevel dc–dc power converter in the presence of failures and normal conditions presented in Section 2, this section presents the main simulation results obtained with the developed model in the PSIM software. These results are presented as a complement of the results obtained in the experimental validation. As aforementioned, this paper considers three different failures in bipolar dc grid: (i) a failure in the positive wire, where v_{dc1} is 0 V and v_{dc2} is 75 V; (ii) a failure in the negative wire, where v_{dc1} is 75 V and v_{dc2} is 0 V; and (iii) a failure in the neutral wire, where the total voltage v_{dc1} and v_{dc2} is 150 V. Moreover, the selected LC filter has a capacitance value of 20 μ F and an inductance value of 700 μ H. Considering a reference current of 4 A, a sampling frequency of 40 kHz, and a switching frequency of 20 kHz, the following simulation results illustrate the operation of the multilevel dc–dc power converter under normal and fault conditions.

Figure 7 shows the transition time from operation under normal conditions to the occurrence of a failure in the positive wire of the bipolar dc grid. Initially, the multilevel dc–dc power converter is operating normally, where the EV battery current (i_{ev}) is in accordance with the reference current, and the ripple presents a frequency that is twice the switching frequency: i.e., 40 kHz. In the beginning, as the multilevel dc–dc power converter operates under normal conditions, the current in the positive wire of the dc grid (i_{pos}) is approximately 2 A. Moreover, the semiconductors S_1 and S_4 are switching, with a duty cycle of about 40%, which results in an EV battery voltage of 60 V. When the current flows through S_1 and the antiparallel diode of S_3 or when the current flows through the antiparallel diode of S_2 and the semiconductor S_4 , the output voltage of the multilevel dc–dc power converter (v_{conv}) is 75 V, i.e., a value that corresponds to $+v_{dc}/2$. When the current flows through the antiparallel diodes of S_2 and S_3 , the EV battery is charged through the inductors L_1 and L_2 , and the voltage value of v_{conv} is 0 V. At 0.005 s, a failure occurs in the positive wire of the bipolar dc grid, where the current i_{pos} is 0 A, and S_1 stops switching. In this case, it is only S_4 that is switched, resulting in an i_{ev} with a ripple whose frequency is 20 kHz (i.e., a value that is half of that obtained under normal conditions). For this reason, the ripple of i_{ev} in the presence of a failure is higher than in normal conditions. Moreover, the duty cycle of S_4 is double that verified in normal conditions. Thus, despite the occurrence of this failure, the current i_{ev} is in accordance with the established reference current, and the voltage v_{ev} maintains its value of 60 V. During the failure in the positive wire of the bipolar dc grid, the two possible operation modes are illustrated in Figure 5a,d.

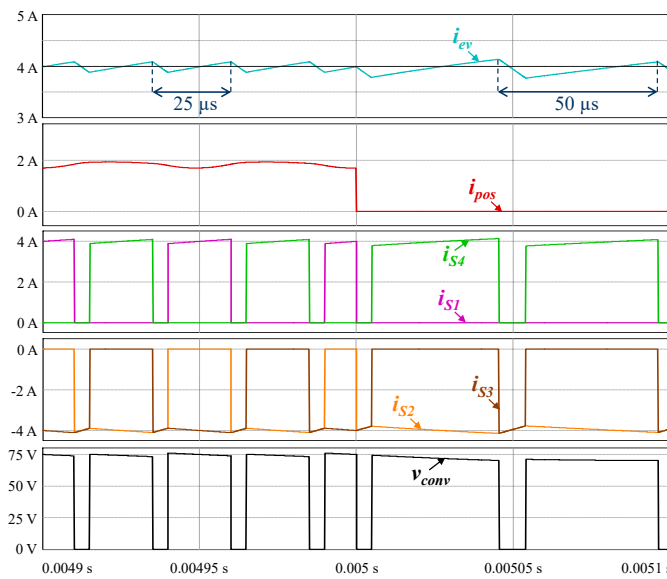


Figure 7. Waveforms of the EV current (i_{ev}), dc grid current in the positive wire (i_{pos}), currents in the IGBTs S_1, S_2, S_3, S_4 ($i_{S1}, i_{S2}, i_{S3}, i_{S4}$), and voltage produced by the dc–dc converter (v_{conv}) during the transition from normal operation to operation with a failure in the positive wire of the bipolar dc grid.

Figure 8 shows the transition time from operation under normal conditions to the occurrence of a failure in the negative wire of the bipolar dc grid. At 0.01502 s, a failure occurs in the negative wire of the bipolar dc grid, where it can be observed that the current in that wire (i_{neg}) is 0 A. Moreover, the voltage v_{dc2} is 0 V, and S_4 is not switching; thus, two possible operation modes in the occurrence of a failure in the negative wire of the bipolar dc grid are illustrated in Figure 5b,d. Since only S_4 is switching, the frequency of ripple of the current i_{ev} is equal to the switching frequency: i.e., 20 kHz. Therefore, the ripple of the current i_{ev} is higher than that observed in normal conditions. However, the current i_{ev} remains the same as the established reference current, and the voltage v_{ev} maintains its value of 60 V.

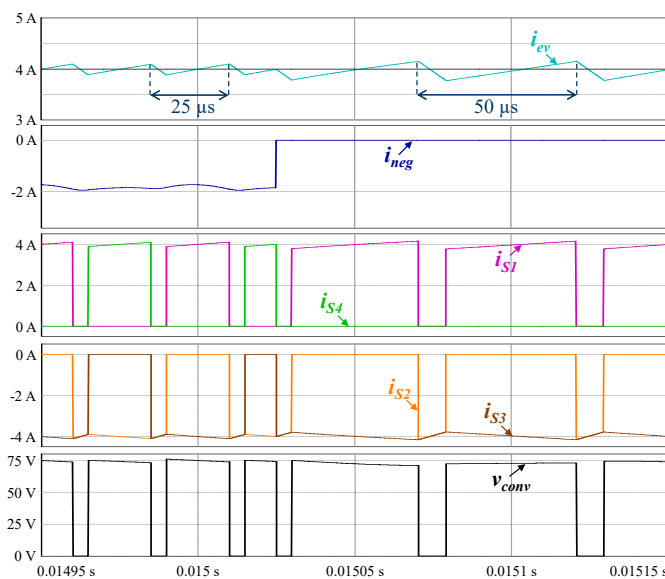


Figure 8. Waveforms of the EV current (i_{ev}), dc grid current in the positive wire (i_{pos}), currents in the IGBTs S_1, S_2, S_3, S_4 ($i_{S1}, i_{S2}, i_{S3}, i_{S4}$), and voltage produced by the dc–dc converter (v_{conv}) during the transition from normal operation to operation with a failure in the negative wire of the bipolar dc grid.

Figure 9 presents the transition time from operation under normal conditions to the occurrence of a failure in the neutral wire of the bipolar dc grid. In normal conditions, the current in the neutral wire (i_N) has an ac component with an average value of 0 A, whereas in the presence of a failure in the neutral wire of the bipolar dc grid, the current i_N is 0 A. Due to the presence of this failure, the ripple of the current i_{ev} is higher than in normal conditions since the frequency of the ripple of the current i_{ev} is equal to the switching frequency: i.e., 20 kHz. Another aspect is the voltage produced by the multilevel dc–dc power converter, since in normal conditions, the voltage v_{conv} varies between 0 V and 75 V ($+v_{dc}/2$), whereas in the occurrence of a failure in the neutral wire of the bipolar dc grid, the voltage v_{conv} assumes the values 0 V and 150 V ($+v_{dc}$). This can be explained by the analysis shown in Figure 5c,d. In Figure 5c, the current flows through the capacitors C_1 and C_2 and the semiconductors S_1 and S_4 , so the voltage v_{conv} is $+v_{dc}$. In Figure 5d, the current flows through the antiparallel diodes of S_2 and S_3 , so the voltage v_{conv} is 0 V.

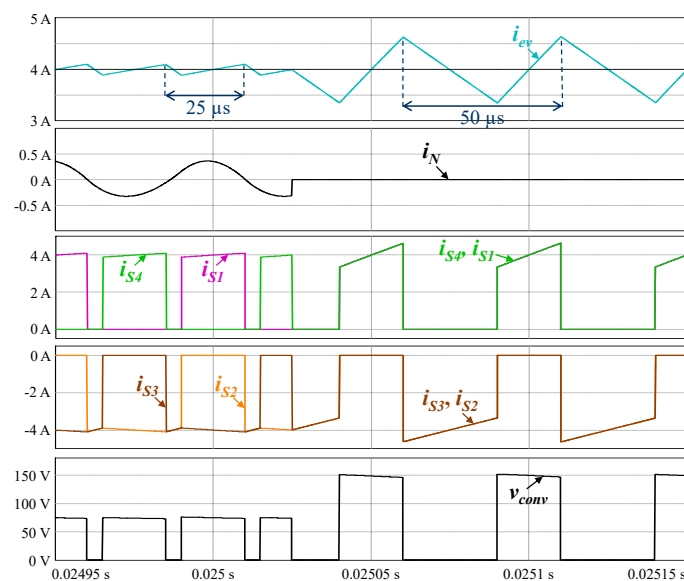


Figure 9. Waveforms of the EV current (i_{ev}), dc grid current in the positive wire (i_{pos}), currents in the IGBTs S_1 , S_2 , S_3 , S_4 (i_{S1} , i_{S2} , i_{S3} , i_{S4}), and voltage produced by the dc–dc converter (v_{conv}) during the transition from normal operation to operation with a failure in the neutral wire of the bipolar dc grid.

4. Experimental Validation

This section describes the laboratory prototype that was developed to validate the bidirectional multilevel dc–dc power converter as an EV battery charger when operating under fault conditions. Figure 10 shows the developed control board, which is composed of eight-channel analog-to-digital converters (ADCs), four pulse-width modulation channels, a microcontroller connection, a digital-to-analog converter with serial peripheral interface (SPI), and a serial port. The eight-channel ADC receives the signals from the voltage and current sensors, and these signals are subsequently adequate to the range of values (0 V to 3.3 V) allowed by the digital signal processor (DSP), whose DSP is the model TMS320F28335 from Texas Instruments. The experimental results were obtained with a Tektronix digital oscilloscope, model TPS2024B.

Figure 11 shows the developed laboratory prototype, which consists of the multilevel dc–dc power converter, the dc-link capacitors, the control board, the DSP docking station, and the Hall effect voltage and current sensors. The multilevel dc–dc power converter is composed of IGBT modules, IGBT drivers, and dc-link capacitors. The dc-link is composed of 25- μ F and 1100-V capacitors, and both the IGBT modules and IGBT drivers are from SEMIKRON, whose references are SKM50GB063D and SKHI22AH4R, respectively. On the other hand, the docking station board of Texas Instruments, TMDSDOCK28335, is used, which allows it to interface with the code composer studio (CCS) software through

a USB port and, thus, debug the implemented code. This section is also divided into two subsections, in which the experimental results of the multilevel dc–dc power converter under normal and fault conditions are described. It is important to note that the experimental validation was performed in a laboratory, and to consider that the main goal was to prove and demonstrate the possibility of a bidirectional multilevel dc–dc converter for EV chargers operating under normal and fault conditions. Additionally, for safety reasons, low voltage values were considered.

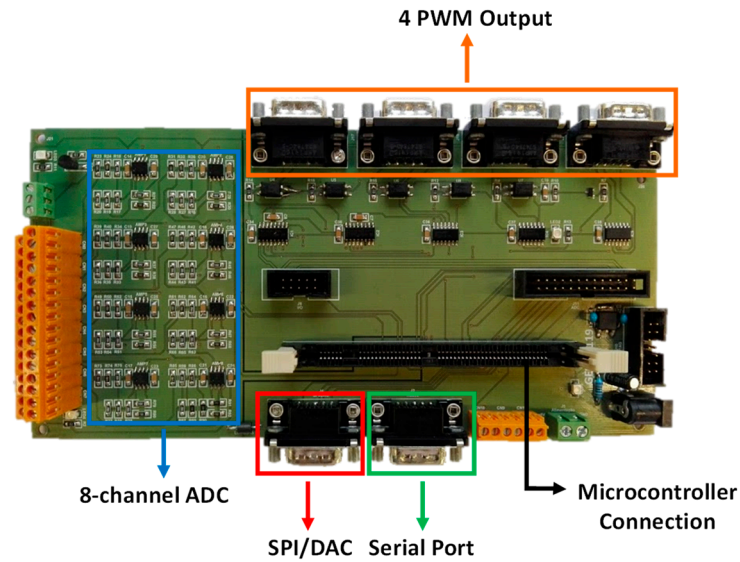


Figure 10. Developed control board of the multilevel dc–dc power converter.

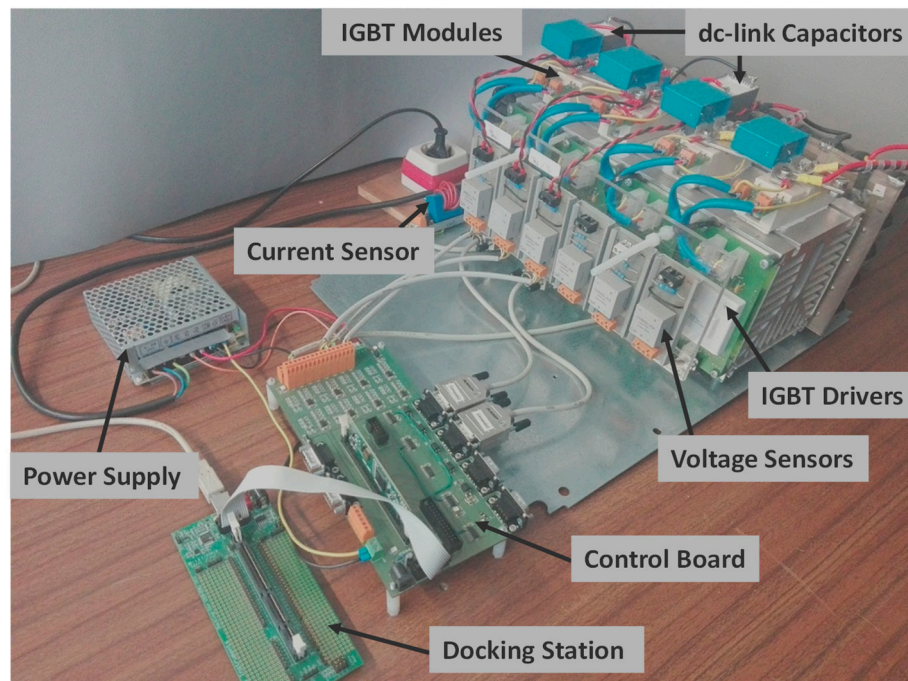


Figure 11. Developed laboratory prototype of the multilevel dc–dc power converter.

4.1. Operation under Normal Conditions

This section presents the experimental results of the multilevel dc–dc power converter operating in normal conditions, i.e., without any failures in the power converter or in the bipolar dc grid. For each experimental result, the EV battery current (i_{ev}) (blue waveform), the external trigger and EV battery voltage (v_{ev}) (both yellow waveforms), and the voltage

between the gate and source of the IGBTs S_1 and S_4 (corresponding to the pink and green waveforms, respectively) are shown. For some experimental results, the voltage v_{ev} was also measured with a Fluke multimeter and a voltage sensor. The external trigger can assume the values 0 V and 3.3 V, and it is used to identify whether there is any failure in the positive, neutral, or negative wire of the bipolar dc grid. If the external trigger has a value of 3.3 V, this indicates that there is a failure in one of the wires of the bipolar dc grid. Otherwise, the multilevel dc–dc power converter is operating in normal conditions.

The experimental validation was carried out considering an input voltage (v_{dc}) of 150 V; i.e., the values of the voltages v_{dc1} and v_{dc2} were 75 V, and an EV battery current was 4 A. Figure 12a,b shows the EV battery charging during normal conditions of operation. In Figure 12a, the current i_{ev} is 4 A and the voltage gate–source of the semiconductors S_1 and S_4 has a duty cycle of 39%; thus, the voltage v_{ev} has a value of about 60 V. In this case, the trigger value is 0 V, which indicates that the multilevel dc–dc power converter is operating normally. Figure 12b shows, in detail, the current (i_{ev}) ripple value, which has a value of 800 mA. This value is compared with the ripple value of the current i_{ev} obtained in the fault conditions, presented in Section 4.2.

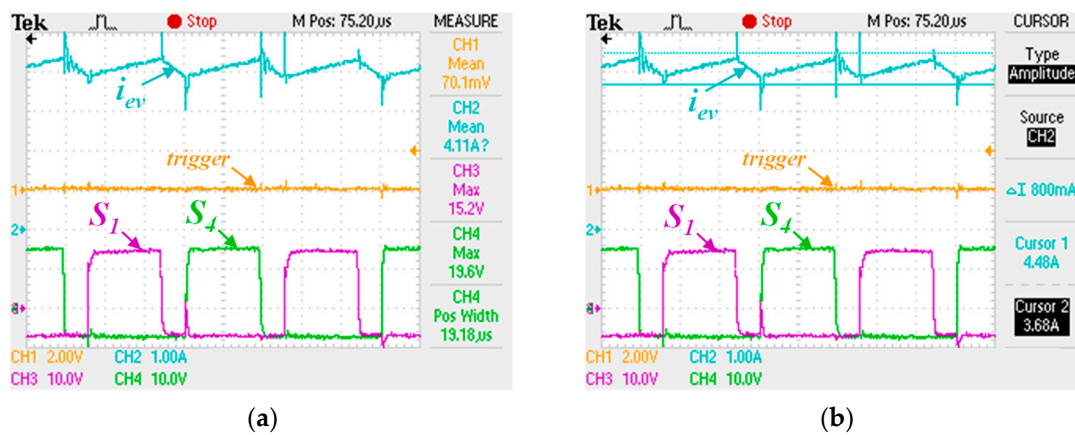


Figure 12. Steady-state operation of the multilevel dc–dc converter under normal conditions: (a) an i_{ev} of 4 A and a duty cycle of 39% for semiconductors S_1 and S_4 ; (b) an i_{ev} ripple value of 800 mA and a trigger value of 0 V.

To validate the operation of the multilevel dc–dc power converter, different input voltage values and a reference current were established to charge the EV battery. In this case, a dc-link voltage of 180 V was established, which corresponds to v_{dc1} and v_{dc2} values of 90 V, and a reference current of 5 A. Figure 13a,b presents the experimental results of the multilevel dc–dc power converter operating under normal conditions. As can be observed in Figure 13a, the current i_{ev} is 5 A, and the semiconductors S_1 and S_4 are switching, which indicates that the dc–dc power converter is operating in normal conditions. Another indicator of the absence of failures in the bipolar dc grid is the external trigger value being 0 V. Figure 13b shows in detail the ripple in the current i_{ev} , whose value is 800 mA. Another observation is the duty cycle value of 39% for S_1 and S_4 , which corresponds to a voltage v_{ev} of approximately 60 V. As aforementioned, these experimental results were compared with the experimental results under fault conditions (presented in the next subsection), in an attempt to analyze the performance of the multilevel dc–dc power converter under both normal and fault conditions.

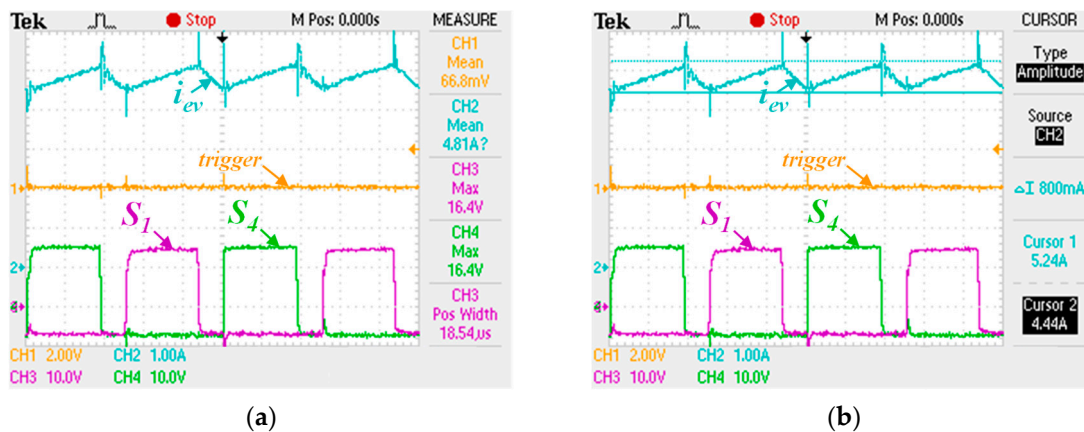


Figure 13. Steady-state operation of the multilevel dc–dc converter under normal conditions: (a) an i_{ev} of 5 A and a duty cycle of 39% for semiconductors S_1 and S_4 ; (b) an i_{ev} ripple value of 800 mA and a trigger value of 0 V.

4.2. Operation under Fault Conditions

After the validation of the multilevel dc–dc power converter under normal conditions, it is important to analyze its operation under fault conditions. As previously mentioned, the multilevel dc–dc power converter was tested in the presence of three different failures in the bipolar dc grid: (i) a failure in the positive wire; (ii) a failure in the negative wire; and (iii) a failure in the neutral wire of the bipolar dc grid.

Figure 14 presents the steady-state operation of the multilevel dc–dc power converter under a failure in the positive wire of the bipolar dc grid. Due to the presence of this failure, the voltage v_{dc1} has a value of 0 V and the voltage v_{dc2} maintains its value of 75 V. Figure 14a shows the transition between normal and faulty conditions following a failure in the positive wire of the bipolar dc grid. This transition can be verified through the change in the trigger value from 0 V and 3.3 V. Moreover, when the trigger value reaches 3.3 V, the semiconductor S_1 stops switching and the semiconductor S_4 continues switching. However, as can be observed from Figure 14a–b, the duty cycle value of S_4 changes. In normal conditions, the duty cycle value of S_4 is 39%, and under fault conditions the duty cycle value increases to 79%. Despite that, the value of the voltage v_{ev} is the same as that verified under normal conditions: i.e., 60 V. Figure 14b shows the ripple value of the current i_{ev} , which is 1 A, greater than that obtained under normal conditions.

Figure 15a shows the transient-state operation from normal conditions to fault conditions; namely, a failure in the negative wire of the bipolar dc grid. During this transition, it is possible to identify the change in the trigger value (to 3.3 V), which indicates the presence of the failure. On the other hand, the presence of a failure in the negative wire of the bipolar dc grid can be identified through the behavior of the semiconductor S_4 . In this case, S_4 stops switching, whereas the duty cycle of S_1 continues switching despite changing from 39% to 71%, which corresponds to a voltage (v_{ev}) value of approximately 60 V. This situation can be observed from Figure 15a–b. Another aspect to consider is the current ripple value of i_{ev} , as demonstrated in Figure 15c, whose value is 1.08 A, a value higher than that verified in normal conditions.

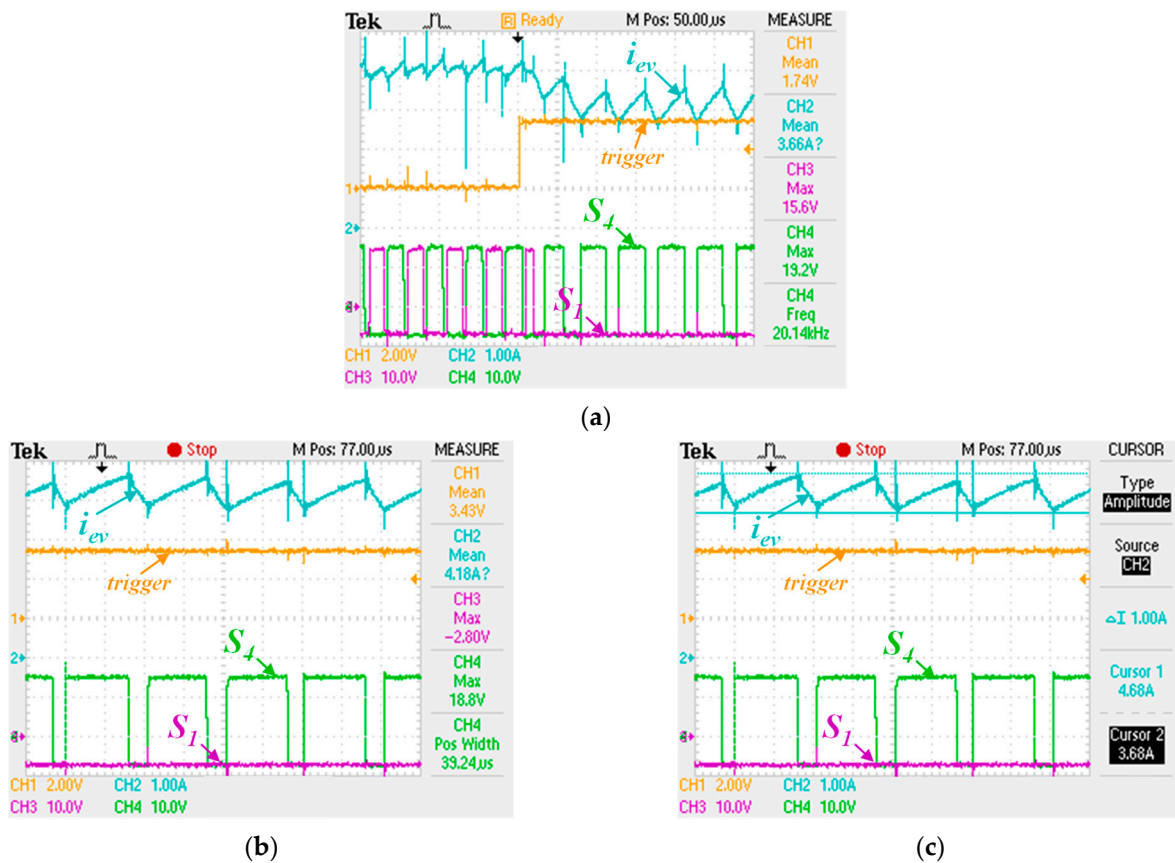


Figure 14. Transient-state operation of the multilevel dc–dc converter after a failure in the positive wire of the bipolar dc grid: (a) transition time from normal conditions (trigger value of 0 V) to fault conditions (trigger value of 3.3 V); (b) an i_{ev} of 4 A and a duty cycle of 0% for semiconductors S_1 , and 79% for semiconductors S_4 ; (c) an i_{ev} ripple value of 1 A.

The multilevel dc–dc power converter’s operation in the presence of a failure in the neutral wire of the bipolar dc grid is presented in Figure 16. The total dc-link voltage is 150 V, so the voltages v_{dc1} and v_{dc2} are both 75 V. In Figure 16a, it is demonstrated that the current i_{ev} equals the reference current of 4 A and has a voltage v_{ev} of 55 V, which corresponds to a S_1 duty cycle value of 38%. However, due to the presence of the failure in the neutral wire of the bipolar dc grid, S_4 is always enabled. Despite the presence of the failure, the current i_{ev} equals the reference current but has a ripple value of 2.16 A, as shown in Figure 16b. The ripple value matches the simulation results previously described, whose ripple value is obtained since the ripple frequency and the switching frequency are the same (20 kHz).

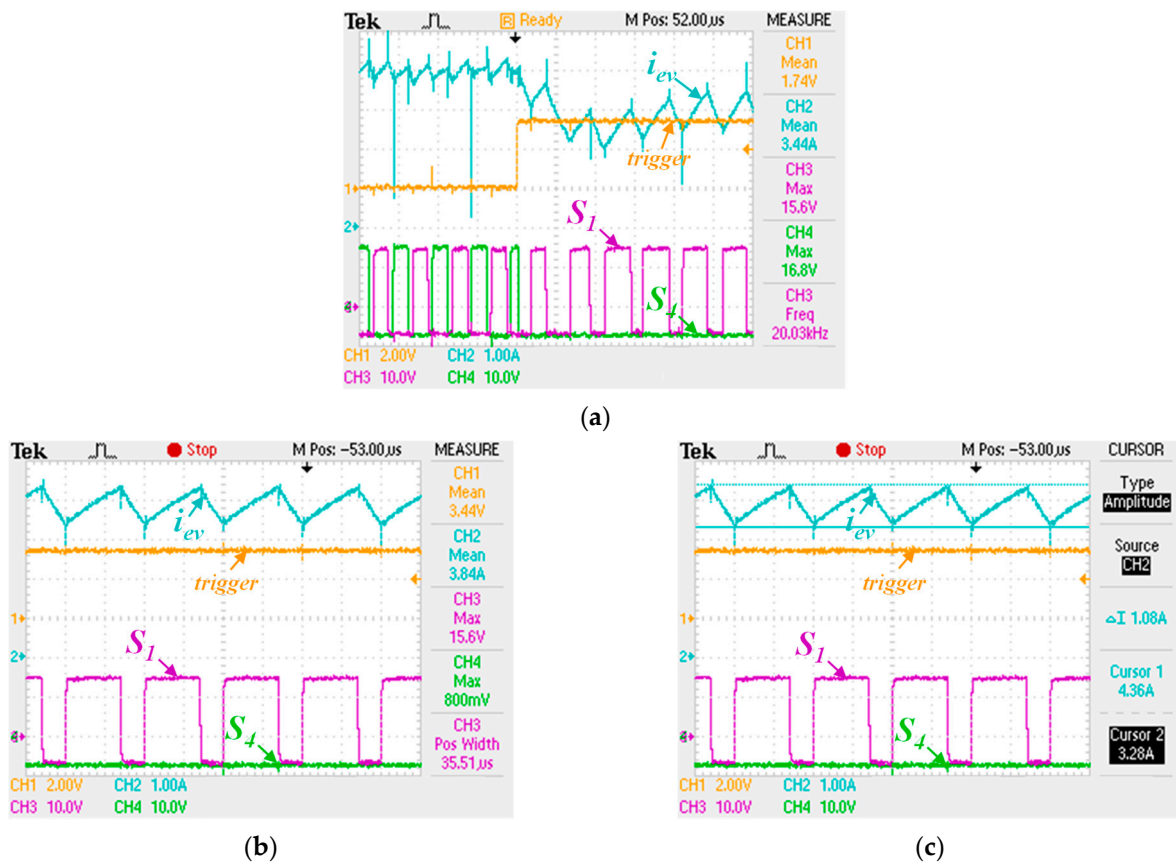


Figure 15. Transient-state operation of the multilevel dc–dc converter following a failure in the negative wire of the bipolar dc grid: (a) transition time from normal conditions (trigger value of 0 V) to fault conditions (trigger value of 3.3 V); (b) an i_{ev} of 4 A and a duty cycle of 71% for semiconductor S_1 , while that of S_4 equals to 0%; (c) an i_{ev} ripple value of 1.08 A.

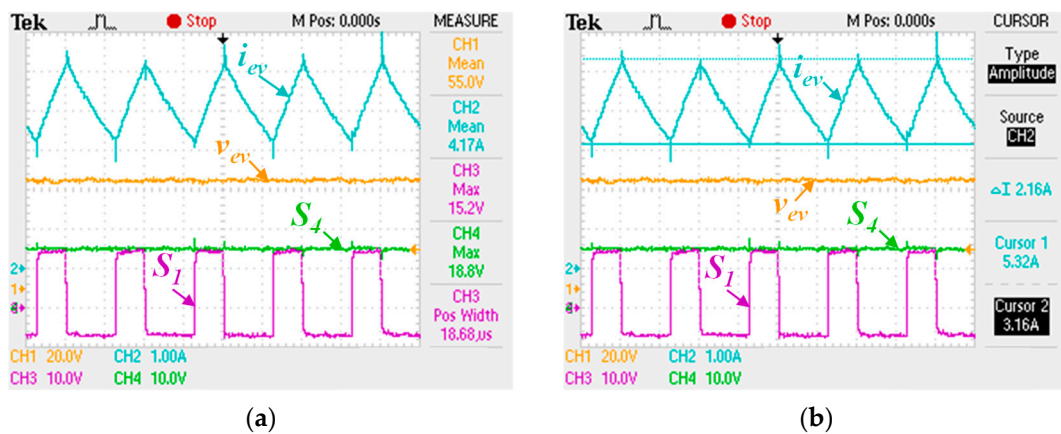


Figure 16. Steady-state operation of the multilevel dc–dc converter following a failure in the neutral wire of the bipolar dc grid: (a) an i_{ev} of 4 A and a v_{ev} of 55 V; (b) an i_{ev} ripple value of 2.16 A and a duty cycle of 38% for S_1 , while that of S_4 is equal to 100%.

Figure 17 demonstrates the steady-state operation of the multilevel dc–dc power converter in the presence of a failure in the positive wire of the bipolar dc grid for a reference current of 5 A. In this case, the dc-link voltage ($+v_{dc}$) is 90 V; i.e., it has a voltage $+v_{dc1}$ of 0 V and a voltage $+v_{dc2}$ of 90 V. Figure 17a shows the transition from normal conditions to the fault condition, where the external trigger changes from 0 V to 3.3 V. As previously mentioned, in the presence of a failure in the positive wire of the bipolar dc grid, there is no current flowing through the semiconductor S_1 and there is only one semiconductor that is switching: namely, the semiconductor S_4 . Moreover, the value of the duty cycle of S_4 increases to 77%, which corresponds to double the value of the duty cycle verified in normal conditions. This situation can be observed from Figure 17a–b. In Figure 17c, it can be observed the value of the current ripple of i_{ev} , despite being higher than obtained in normal conditions, is slightly higher than verified in the fault case operation.

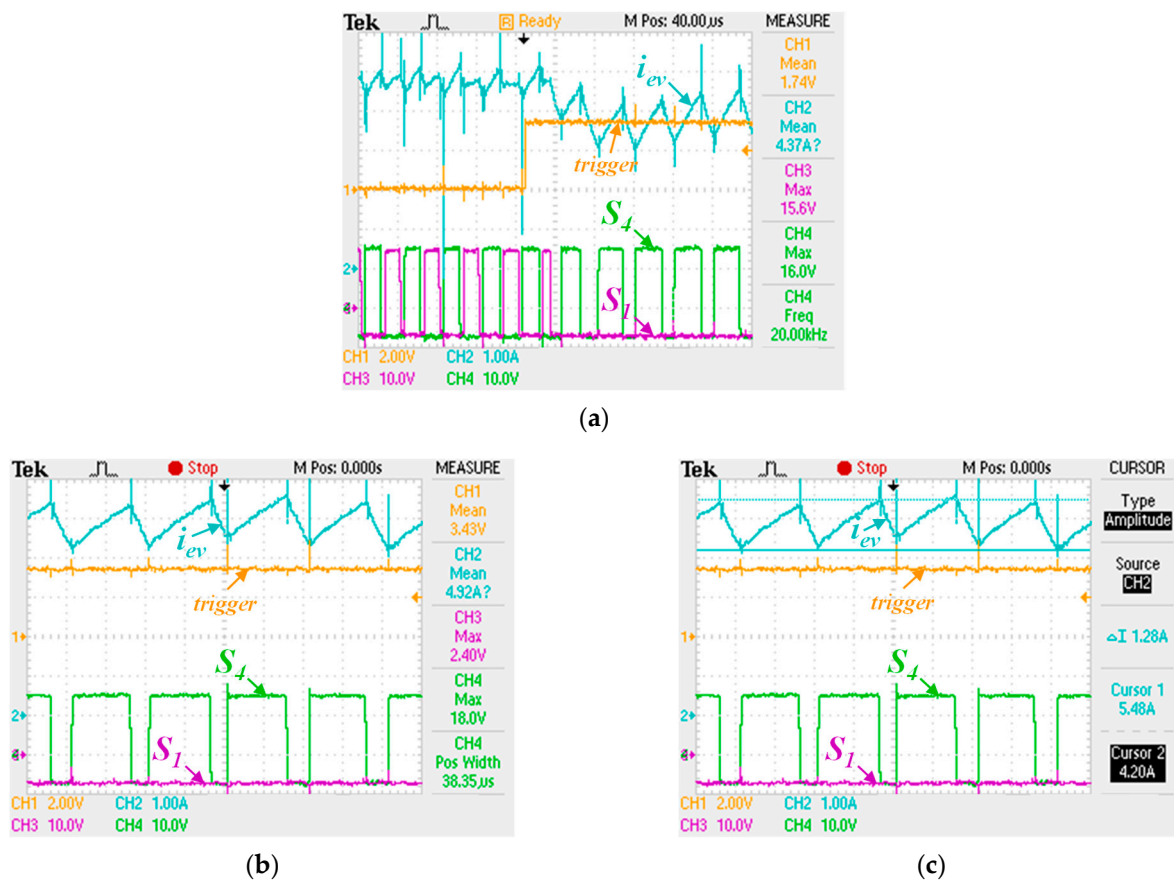


Figure 17. Transient-state operation of the multilevel dc–dc converter following a failure in the positive wire of the bipolar dc grid: (a) transition time from normal conditions (trigger value of 0 V) to fault conditions (trigger value of 3.3 V); (b) an i_{ev} of 5 A and a duty cycle of 0% for semiconductor S_1 and 77% for semiconductor S_4 ; (c) an i_{ev} ripple value of 1.28 A.

The multilevel dc–dc power converter operation in the presence of a failure in the negative wire of the bipolar dc grid, for a reference current of 5 A, is presented in Figure 18. Due to the presence of the failure, the voltage v_{dc2} is 0 V and the voltage v_{dc1} maintains a voltage value of 90 V. As there is no current through the semiconductor S_4 ; it is only the semiconductor S_1 that is switching, and thus the value of the current ripple of i_{ev} is higher than in normal conditions. This situation can be observed from Figure 18a–b. Figure 18c shows in more detail the value of the current ripple of i_{ev} , whose value is slightly higher than that verified in the similar case previously presented.

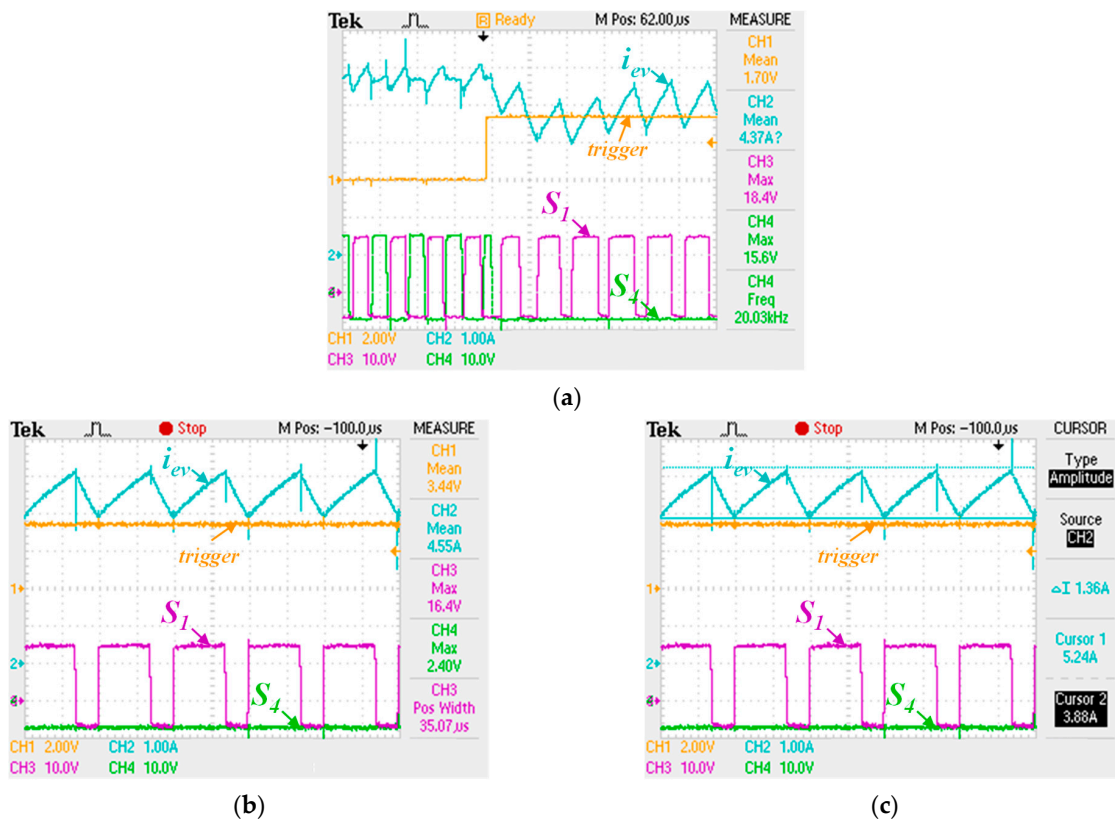


Figure 18. Transient-state operation of the multilevel dc–dc converter following a failure in the negative wire of the bipolar dc grid: (a) transition time from normal conditions (trigger value of 0 V) to fault conditions (trigger value of 3.3 V); (b) an i_{ev} of 5 A and a duty cycle of 70% for semiconductor S_1 , while that of S_4 is equal to 0%; (c) an i_{ev} ripple value of 1.36 A.

Figure 19 presents the steady-state operation of the multilevel dc–dc power converter following a failure in the neutral wire of the bipolar dc grid, for a reference current of 5 A. Despite the presence of this failure, the current i_{ev} is equal to the reference current, and a voltage v_{ev} of 66.4 V is obtained, which corresponds to 37% of the dc-link voltage (180 V). Additionally, S_1 is switching and S_4 is always enabled. Figure 19b shows the ripple value of the current i_{ev} , whose value is still considerable (2.64 A). This same value was obtained previously, as demonstrated in Figure 19; however, the ripple value is slightly higher since the established reference current, as well as the dc-link voltage, is also higher.

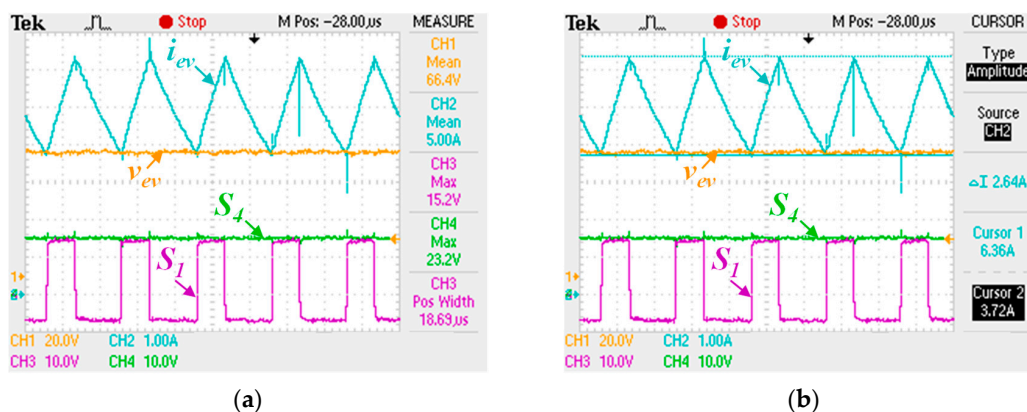


Figure 19. Steady-state operation of the multilevel dc–dc converter following a failure in the neutral wire of the bipolar dc grid: (a) an i_{ev} of 5 A and a v_{ev} of 66.4 V; (b) an i_{ev} ripple value of 2.64 A and a duty cycle of 37% for S_1 , while that of S_4 is equal to 100%.

5. Conclusions

This paper presents, analyses, and experimentally validates the operation of a developed bidirectional multilevel dc–dc power converter for an EV battery charger operating under normal conditions and in the presence of faults, which can occur in the power grid. The dc–dc power converter was designed to integrate with the EV battery and a bipolar dc grid, where three different failures can occur; namely, a failure in the positive wire, in the negative wire, or in the neutral wire. As was demonstrated in this paper, both in normal conditions and in the presence of a failure in the bipolar dc grid, the dc–dc power converter must guarantee the correct EV battery-charging operation. In light of this, a considerable set of simulation and experimental results are presented to illustrate the EV battery-charging operation, both during normal and fault conditions, validating the topology of the power converter, as well as the proposed control algorithms. The experimental validation was performed considering real scenarios of open-circuit failures on the bipolar dc grid that supplies the bidirectional multilevel dc–dc power converter. Moreover, the experimental validation was performed considering validation both in a steady state and a transient state. Under normal conditions, considering the proposed interleave-based control strategy, the EV battery current presents a ripple with a frequency that corresponds to double the switching frequency. This is a low ripple value, which represents an important advantage of this multilevel dc–dc converter. Considering the ripple of the current, this operation is comparable to a traditional dc–dc interleaved converter, however, adding the voltage multilevel feature of the dc–dc power converter. The addition of this feature is an important advantage, as demonstrated throughout this paper. Moreover, in the presence of a failure in the positive, negative, or neutral wire of the bipolar dc grid, the multilevel dc–dc converter can change its operation to avoid an interruption in the charging process. It is important to note that this situation is only possible in this multilevel dc–dc converter, which presents interleaved and multilevel features, and offers the possibility of operating in the presence of failures on the bipolar dc grid. In such a situation, the ripple of the EV battery current is higher than verified in normal conditions, but even so, the EV charging process is not interrupted, which is a very important feature that was experimentally validated in this paper. This is explained by the fact that under fault conditions, the EV battery current frequency is equal to the switching frequency (no longer double), since only one semiconductor is operating. Despite that, even in the presence of a failure, the EV battery current is controlled according to the established reference current, thus ensuring the correct EV battery-charging operation. Such operational ability is very important, however, without the interleaved and multilevel features, which are restored when the failures are fixed. This situation is not allowed by traditional dc–dc power converters, where the EV battery-charging process is interrupted in the case of a failure in any wire of the power grid. Several experimental results are presented for the different conditions of operation, which were obtained with a developed laboratory prototype, validating the proposed control algorithms and the features of the multilevel dc–dc power converter operating as EV battery charger, both under normal and fault conditions, as well as in a steady state and in a transient state.

Author Contributions: Conceptualization, V.M.; validation, C.F.O.; writing—original draft preparation, C.F.O. and V.M.; writing—review and editing, C.F.O., V.M. and J.L.A.; supervision, V.M. All authors have read and agreed to the published version of the manuscript.

Funding: This work has been supported by FCT-Fundação para a Ciência e Tecnologia within the R&D Units Project Scope: UIDB/00319/2020. This work has been supported by the MEGASOLAR Project POCI-01-0247-FEDER-047220.

Conflicts of Interest: The authors declare no conflict of interest.

References

1. Sharma, G.; Sood, V.; Alam, M.; Shariff, S. Comparison of common DC and AC bus architectures for EV fast charging stations and impact on power quality. *ETransportation* **2020**, *5*, 100066.
2. Leone, C.; Longo, M.; Fernández-Ramírez, L.M. Optimal Size of a Smart Ultra-Fast Charging Station. *Electronics* **2021**, *10*, 2887.
3. Monteiro, V.; Afonso, J. A Unified Topology for the Integration of Electric Vehicle, Renewable Energy Source, and Active Filtering for the Power Quality Improvement of the Electrical Power Grid: An Experimental Validation. *Electronics* **2022**, *11*, 429.
4. Montoya, O.; Garrido, V.; Gil-González, W.; Grisales-Noreña, L. Power flow analysis in DC grids: Two alternative numerical methods. *Trans. Circuits Syst. II Express Briefs* **2019**, *66*, 1865–1869.
5. Jiya, I.; Khang, H.; Kishor, N.; Ciric, R. Novel Family of High-Gain Nonisolated Multiport Converters with Bipolar Symmetric Outputs for DC Microgrids. *Trans. Power Electron.* **2022**, *37*, 12151–12166. [[CrossRef](#)]
6. Chandra, A.; Singh, G.; Pant, V. Protection techniques for DC microgrid- A review. *Electr. Power Syst. Res.* **2020**, *187*, 106439.
7. Zhao, S.; Chen, Y.; Cui, S.; Hu, J. Modular Multilevel DC-DC Converter With Inherent Bipolar Operation Capability for Resilient Bipolar MVDC Grids. *CPSS Trans. Power Electron. Appl.* **2022**, *7*, 37–48. [[CrossRef](#)]
8. Jarrahi, M.; Roozitalab, F.; Arefi, M.; Javadi, M.; Catalao, J. Dc microgrid energy management system containing photovoltaic sources considering supercapacitor and battery storages. In Proceedings of the 2020 International Conference on Smart Energy Systems and Technologies (SEST), Istanbul, Turkey, 7–9 September 2020; pp. 1–6.
9. Metwly, M.; Abdel-Majeed, M.; Abdel-Khalik, A.; Hamdy, R.; Hamad, M.; Ahmed, S. A review of integrated on-board EV battery chargers: Advanced topologies, recent developments and optimal selection of FSCW slot/pole combination. *Access* **2020**, *8*, 85216–85242.
10. Monteiro, V.; Lima, P.; Sousa, T.; Martins, J.; Afonso, J. An off-board multi-functional electric vehicle charging station for smart homes: Analysis and experimental validation. *Energies* **2020**, *13*, 1864. [[CrossRef](#)]
11. Ali, A.; Chuanwen, J.; Yan, Z.; Habib, S.; Khan, M. An efficient soft-switched vienna rectifier topology for EV battery chargers. *Energy Rep.* **2021**, *7*, 5059–5073. [[CrossRef](#)]
12. Monteiro, V.; Pinto, J.; Afonso, J. Improved vehicle-for-grid (iV4G) mode: Novel operation mode for EVs battery chargers in smart grids. *Int. J. Electr. Power Energy Syst.* **2019**, *110*, 579–587. [[CrossRef](#)]
13. Schäfer, J.; Kolar, J. Three-Port Series-Resonant DC/DC Converter for Automotive Charging Applications. *Electronics* **2021**, *10*, 2543.
14. Arif, S.; Lie, T.; Seet, B.; Ayyadi, S.; Jensen, K. Review of Electric Vehicle Technologies, Charging Methods, Standards and Optimization Techniques. *Electronics* **2021**, *10*, 1910.
15. Gaona-Cárdenas, L.-F.; Vázquez-Nava, N.; Ruíz-Martínez, O.-F.; Espinosa-Calderón, A.; Barranco-Gutiérrez, A.-I.; Rodríguez-Licea, M.-A. An Overview on Fault Management for Electric Vehicle Onboard Chargers. *Electronics* **2022**, *11*, 1107. [[CrossRef](#)]
16. Balasundar, C.; Sundarabalan, S.; Sharma, J.; Srinath, J.; Guerrero, J. Effect of Fault Ride Through Capability on Electric Vehicle Charging Station Under Critical Voltage Conditions. *Trans. Transp. Electrification* **2022**, *8*, 2469–2478.
17. Bento, F.; Cardoso, A. Fault tolerant DC-DC converters in DC microgrids. In Proceedings of the 2017 IEEE Second International Conference on DC Microgrids (ICDCM), Nuremberg, Germany, 27–29 June 2017; pp. 484–490.
18. Wen, H.; Li, J.; Shi, H.; Hu, Y.; Yang, Y. Fault Diagnosis and Tolerant Control of Dual-Active-Bridge Converter with Triple-Phase Shift Control for Bidirectional EV Charging Systems. *Trans. Transp. Electrification* **2021**, *7*, 287–303.
19. Kaler, S.; Yazdani, A. A DC-Side Fault-Tolerant Bidirectional AC-DC Converter for Applications in Distribution Systems. *Access* **2022**, *10*, 46608–46617.
20. Wang, Y.; Guan, Y.; Molinas, M.; Fosso, O.; Hu, W.; Zhang, Y. Open-Circuit Switching Fault Analysis and Tolerant Strategy for Dual-Active-Bridge DC-DC Converter Considering Parasitic Parameters. *Trans. Power Electron.* **2022**, *37*, 15020–15034. [[CrossRef](#)]
21. Caseiro, L.; Mendes, A. Fault Analysis and Non-Redundant Fault Tolerance in 3-Level Double Conversion UPS Systems Using Finite-Control-Set Model Predictive Control. *Energies* **2021**, *14*, 2210.
22. Kumar, G.; Elangovan, D. Review on fault-diagnosis and fault-tolerance for DC-DC converters. *Power Electron.* **2020**, *13*, 1–13.
23. Bhargav, R.; Bhalja, B.; Gupta, C. Novel fault detection and localization algorithm for low-voltage dc microgrid. *Trans. Ind. Inform.* **2019**, *16*, 4498–4511.
24. Zhuo, S.; Xu, L.; Gaillard, A.; Huangfu, Y.; Paire, D.; Gao, F. Robust open-circuit fault diagnosis of multi-phase floating interleaved DC-DC boost converter based on sliding mode observer. *Trans. Transp. Electrification* **2019**, *5*, 638–649. [[CrossRef](#)]
25. Zhuo, S.; Gaillard, A.; Xu, L.; Liu, C.; Paire, D.; Gao, F. An Observer-Based Switch Open-Circuit Fault Diagnosis of DC-DC Converter for Fuel Cell Application. *Trans. Ind. Appl.* **2020**, *56*, 3159–3167.
26. Givi, H.; Farjah, E.; Ghanbari, T. Switch and Diode Fault Diagnosis in Nonisolated DC-DC Converters Using Diode Voltage Signature. *Trans. Ind. Electron.* **2018**, *65*, 1606–1615. [[CrossRef](#)]
27. Xu, L.; Ma, R.; Xie, R.; Xu, J.; Huangfu, Y.; Gao, F. Open-Circuit Switch Fault Diagnosis and Fault-Tolerant Control for Output-Series Interleaved Boost DC-DC Converter. *Trans. Transp. Electrification* **2021**, *7*, 2054–2066.

28. Bento, F.; Cardoso, A. Open-circuit fault diagnosis and fault tolerant operation of interleaved DC-DC boost converters for homes and offices. *Trans. Ind. Appl.* **2019**, *55*, 4855–4864. [[CrossRef](#)]
29. Leite, R.; Afonso, J.; Monteiro, V. A novel multilevel bidirectional topology for on-board EV battery chargers in smart grids. *Energies* **2018**, *11*, 3453.

Disclaimer/Publisher’s Note: The statements, opinions and data contained in all publications are solely those of the individual author(s) and contributor(s) and not of MDPI and/or the editor(s). MDPI and/or the editor(s) disclaim responsibility for any injury to people or property resulting from any ideas, methods, instructions or products referred to in the content.